

Model-Free Unsupervised Anomaly detection framework in multivariate time-series of industrial dynamical systems

Mazen Alamir^a, Raphaël Dion^a

^aUniv. Grenoble Alpes, CNRS, Grenoble INP, GIPSA-lab, 38000 Grenoble, France.

Abstract

In this paper, a new model-free anomaly detection framework is proposed for time-series induced by industrial dynamical systems. The framework lies in the category of conventional approaches which enable appealing features such as, a fast learning with reduced amount of learning data, a reduced memory, a high potential for explainability as well as easiness of incremental learning mechanism to incorporate operator feedback after an alarm is raised and analyzed. All these are crucial features towards acceptance of data-driven solution by industry but they are rarely considered in the comparisons between competing methods which generally exclusively focus on performance metrics. Moreover, the features engineering step involved in the proposed framework is inspired by the time-series being implicitly governed by physical laws as it is generally the case in industrial time-series. Two examples are given to assess the efficiency of the proposed approach.

Keywords: Model Predictive Control, Nonlinear Systems, Short Prediction Horizon

1. Introduction

Model-free anomaly detection in industrial time-series is a major challenge for obvious safety and economic reasons. This challenge is even harder to tackle in the unsupervised setting, namely, when the model used in the decision process is to be built based on healthy time-series only and in the absence of any mathematical knowledge-based model.

It is a fact that this setting is the only realistic one in many industrial contexts where no mathematical models are available and given the scarcity of *labelled* anomalous instances that can hardly cover all possible deviations from normality.

The absence of a mathematical model describing the equations that govern the industrial equipment time-series and their cross-correlations excludes the design of dynamic observers. This is the reason why observer-based anomaly detection methodologies are not analyzed in the present contribution.

To be more specific, the paradigm of model-free unsupervised anomaly detection in time-series can be stated in the following terms:

Use sensors recordings containing healthy time-series to derive an anomaly detector that takes as argument a new time-series (of given length) and produce a diagnosis regarding whether this time-series should be considered as normal or anomalous.

Email addresses: mazen.alamir@grenoble-inp.fr (Mazen Alamir), raphael.dion@grenoble-inp.fr (Raphaël Dion)

Preprint

This topic has attracted a huge amount of work in the last recent years leading to a very rich taxonomy of methods and approaches. The amounts of produced works already fired the need for many survey papers providing a comprehensive categorization (see [8, 4, 5, 24, 23] and the references therein).

In order to position the present contribution in the landscape of possibilities, the consistent classification proposed in [3] is adopted here because of its clarity on one hand and because it solidly brings conclusions (see Section 1.2) that support the family of *conventional* approaches adopted in the present contribution. According to [3], the existing frameworks for the design of anomaly detectors can be divided into three categories (see Figure 1), namely: 1) Conventional methods, 2) Machine learning-based methods and 3) Deep Neural Networks-based methods¹. In the

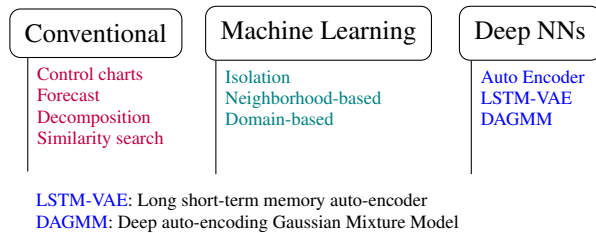


Figure 1: Classification of anomaly detection methods in time-series as suggested by [3].

following section, these categories are briefly described in order to support the discussion of Section 1.2.

1.1. State of the art

Notice that describing a design approach for anomaly detection amounts at explaining how it elaborates *residuals* from *raw sensors data*. The residual is then compared to an elaborated threshold in order to transform the real value into a binary decision. It goes without saying that only a brief and necessarily partial description of the state-of-the-art can be given for each class of approaches in order to grasp the main characteristics and hence to keep a clear view of the *big picture* so that the subtle novelties of the proposed approach can be appreciated. Note also that the way the appropriate threshold is determined once the residual is generated is a crucial step on its own which is common to all the approaches and which is not discussed in the present paper. Further comments on this issue are provided in the conclusion.

1.1.1. Conventional methods

These methods are denoted as *conventional* since they do not involve any Machine Learning step, they can be split into four categories.

In the so-called **control chart**-like approaches, auxiliary variables are generated, using the learning data, by integrating [26] or filtering [16] the excursions (away from the mean values) of some multivariate statistics. Then by characterizing bounds on the resulting excursions, the *normal* range of variations is determined. The residual is then defined to be the distance to the so defined normality region.

In the **forecasting**-based methods, the residual is taken to be the prediction error based on a (generally linear) auto-regressive model that takes the previous values of the sensors as inputs and attempts to predict the next values [15]. Notice that as explained later (Section 1.1.3), the family of auto-encoder based methods also use the prediction errors while using DNNs as the underlying prediction model.

The normality in the **decomposition** methods is defined by the persistent relevance of a reduced dimensional representation of the time-series using different dimensionality reduction paradigms such as: Principal Component Analysis

¹Note that although the last category lies rigorously in the Machine Learning paradigm, the importance of the works dedicated to the Deep Neural Networks (DNNs) and their current burst justifies, according to [3], a specific category on its own.

[25], Singular Spectrum Analysis [30] capturing the main dynamic-related correlations or Independent Component Analysis [20] that are intended to separate independent processes governing the dynamics. In all these cases, the residual is defined by the reconstruction errors of the signal when projected on the lower dimensional subspace.

Finally, in the **similarity** search approaches, the sub-sequences of a time-series are described by matrices of indicators (patterns) and the residuals are defined to be the minimum distances to the elements of a set of matrices representing the normality in the training data [28, 19].

1.1.2. Machine Learning Based methods

These methods share the fact that at some stage, a machine learning tool is used to characterize a sample (that can be a window of raw time-series) as normal or as an outlier. As suggested by [11], this class of methods can be split into three categories, namely: isolation methods, neighborhood-based methods and domain-based methods.

In the **isolation methods**, decision trees are used [14] in order to attempt to isolate the sample from the rest of the data, the lower the number of *cut-off* operations that are needed before isolation is obtained, the higher is the probability that the sample is anomalous.

In the **neighborhood-based** methods, an anomalous measurement is characterized by the low density of its neighbors determined via clustering methods such as K-Nearest neighbors [6] or Density-based spatial clustering of applications with noise (DBSCAN) [13].

Finally, in the **domain-based** approaches, the normality domain (hyper spheres/cubes to cite but two examples) is computed using one-class Support Vector Machine (OC-SVM) and the distance to the resulting domain is considered to be the residual that fires anomalous diagnosis flag when it goes beyond the computed threshold [22].

Notice that these approaches do not exploit the specificity of time-series as they consider a time-series over a window of length n as a point in \mathbb{R}^n . Here, non time-series-specific methods are recycled to handle time-series as a particular example.

1.1.3. Deep Neural Networks based methods

These methods can be grouped in a set of increasingly sophisticated versions of the basic **auto-encoder (AE)** [21] where a specific architecture of a DNN is used involving an intermediate low density layer performing a kind of dimensionality reduction task. The ability to reconstructing, with a good precision, the raw time-series by the remaining part of the DNN out of the resulting *relatively smaller number of features* is a sign of normality². The residual is therefore defined as the reconstruction error. The **unsupervised anomaly detection (USAD)** is a more sophisticated version of the AE in which two AEs are used to play adversarial training game (one of the AEs draw artificial samples to fool the other one) [2]. This enables to enrich the training data while using the same amount of real measurements.

The normality can also be associated to the persistent relevance of some time dependencies characterizing the normal time-series. This is exploited in the so called **long short-term memory variational auto-encoder (LSTM-VAE)** [17].

A recent version of the auto-encoder principle is proposed [31] where the low dimensional compressed intermediate layer is fed into a **Gaussian Mixture Model (GMM)** to build the reconstruction model. The parameters of both the AE and the GMM are optimized in order to reduce the reconstruction error which is used as residual.

1.2. Discussion

In their excellent contribution [3], the authors showed that when comparing up to sixteen anomaly detectors lying in the categories surveyed in Section 1.1 over five known and widely used benchmark problems, a new validation of the *no-free-lunch* theorem [1] clearly appears, namely:

²This recalls the principle of the decomposition methods mentioned in Section 1.1.1

*No family of methods **systematically** outperforms the others [3].*

It also clearly appears that while the DNNs based approaches might slightly better capture some dependencies that are difficult to grasp by the other tested methods, not surprisingly, the performance of these approaches drops quickly when removing a part of the training data. In particular, as far as the involved benchmark problems are concerned, it appears that:

Conventional methods globally obtain better results when the dataset size is less than 50% of the original one [3].

One by-product of the comparison done by [3] is that ML-based solutions seem to be less appropriate to handle time-series specificities. This is not surprising given that time-series instances are seen as simple points in a high dimensional space.

Another widely shared critic regarding DNN-based approaches is the **explainability** issue which is of a tremendous importance in the industrial context we are focusing on in the present paper. It happens that the lack of data is even more critical in this context because of the variety of operational conditions that renders the task of separating anomalies from unseen contexts of use even harder without a huge amount of data should over-parameterized underlying models be used such as the ones involved in DNNs mentioned in the previous section.

Another issue that is almost never represented in the benchmark problems used in the academic works is the difficulty in labelling the industrial time-series. Indeed, the presence of anomalies in the equipments does not mean that these anomalies can be detected in every single window of the time-series (think about a default in the braking device which can be revealed only over those time windows involving braking manoeuvres). In spite of this obvious fact, it is likely that the label provided by the operator would refer to an *anomalous* braking system as soon as the default is detected and until its handling by the maintenance operators and this regardless of braking manoeuvres being undertaken or not. This strongly biases the performance metrics of any model.

Analogously, the early detection of anomalies negatively impacts the measured performance metrics of a model rather instead of being praised for its anticipation of failure [10]. Indeed given the initially provided labels, an early detection increases the rate of *False Positive* instances if the operators switch the label to *anomalous* a bit lately and only once the humanly measurable effects of the default are detected or because of the long periods separating two successive inspection rounds. The consequence of this is that **very good models would be penalized for precisely being good in anticipating the human acknowledgement of the failure.**

Consequently, the last two mentioned labelling problems introduce high bias on the performance metrics when industrial-like time-series and labeling are involved on one hand and more importantly, they underline the importance of **operator feedback handling**. Indeed, the operator feedback is the mechanism by which a careful labelling (or re-labelling) is returned after an alarm is raised to tell the model whether the sample under scrutiny is truly anomalous or not or when a non detected anomaly is discovered by the operators which has been considered by the anomaly detector as normal.

This discussion above brings under light a property of an anomaly detector that is scarcely considered in the commonly provided comparisons while it is tremendously important to the adoption of any algorithm in real-life industry:

***Feedback Friendly Models (FFM):** These are models that can be incrementally changed to take into account an operator feedback regarding the diagnosis of a specific window of time-series.*

It is important to notice that the FFM property is not commonly satisfied by many state-of-the-art models, at least in their officially published versions. The reason is that a feedback returned by an operator generally concerns only

a specific isolated window with a size that is generally negligible when compared to the size of the training data that has been used to *derive the initial version of the model*. Consequently, if one simply re-runs the training step from scratch after adding to the training data the new labelled portion returned by the operator, then because of the relatively extremely small size of the new labelled portion, the impact on the updated model would almost surely be infinitesimal and the operator feedback will not be incorporated appropriately. The almost unchanged anomaly detector will almost surely produce the same erroneous diagnosis under the same conditions. Obviously, simply increasing the computed threshold, each time a False Positive feedback is returned by the maintenance operator, is obviously not the appropriate option as it affect all the samples and not only the ones corresponding to a bad diagnosis.

The above feedback compatibility issue is tightly linked to the concept of *incremental learning* [27] (or batch learning) where the model is regularly updated when a new batch of data is available. The difference here is that the size of the data is not necessarily small compared to the initial training data.

One underlying issue when attempting to address this question is the amount of data that needs to be kept in order to evaluate the impact of model adaptation on the representation of normality. As an example, one can think about a ML domain-based model (Section 1.1.2) that initially computed the normality domain using OC-SVM algorithm. If after a feedback following a False Positive alarm, the boundary of the admissible domain has to be updated accordingly in order to include the new samples in the normality space³, it is mandatory to analyse the impact of this modification on the previously normal instances contained in the original data. If these instances are removed, this analysis would be impossible to do.

1.3. Outline

The remainder of the paper is organized as follows: Section 2 clearly positions the contribution in the landscape of possibilities and underlines the rationale behind the adopted approach. The details of the algorithm are given in Section 3. Some examples are proposed in Section 4, namely two simulated dynamical systems (a parameterized Lorenz oscillator and an automotive controlled electronic angular positioning system). A benchmark against common algorithms on these examples is proposed in Section 5. Finally, Section 6 concludes the paper and gives some suggestions for future investigation to be pursued towards a complete anomaly detection design.

2. Positioning of the proposed anomaly detector

The guiding lines that characterize the proposed anomaly detector can be summarized by the following requirements and items of concerns:

- (1) We seek a design that exploits the **specificity of industrial time-series** that should obey some underlying, although unknown, physical laws. The latter introduce correlations between the *the state vector values, represented by all the available sensors values at some instant* and the possible **time-increments of sensors values**. This is the reason why these increments play a crucial rule in the forthcoming development. Ideally this role should have been played by the time derivatives which is avoided here to come out with a generic solution that holds in the presence of noise but also in order to preserve the computational efficiency in case a large number of sensors are involved.
- (2) In order to fully implement the previous intuition, it is mandatory to come out with a **fully multivariate solution** (by opposition to those solutions that are mainly mono-sensors but which are extended to the multivariate context by simple features concatenation).
- (3) We seek a design that is **robust to sensor incompleteness**. Indeed, in industrial time-series, it is not always the case that all the information that is needed to model the dynamics of the underlying process are included in the available data. This means that predicting the next values of the sensors is frequently not possible if not irrelevant, or to say it differently, far too ambitious for the *anomaly detection task*. One can think about a controlled system

³Which cannot be done by re-running the learning from scratch for the imbalance issue explained earlier!

for which the set-point-like signals are not included in the available data while they obviously determines the future behavior one intends to capture. That is why in the proposed solution, the residual is not based on a reconstruction error of future signals.

(4) In order to address common industrial expectations, a solution with a **high degree of explainability** should be preferred. Typical explanatory sentences might be: "*There is something wrong with sensor i*" or "*something unusual is anomalous when the dynamics of sensor j is high*" or "*sensor i goes beyond its normal domain when sensor j is going down slowly!*" Such additional explanatory hints might not precisely localize the issue but it can greatly help operators to generate working assumptions that can accelerate the diagnosis task.

(5) Last but not least, following the discussion of Section 1.2, we are interested in **Feedback Friendly Models** that enable incremental adaptation of the models parameters as soon as an operator feedback is returned and this while avoiding the need to keep the training data in memory. By the same occasion, such models are naturally compatible with incremental learning as soon as a new bunch of data is made available through new measurements.

The concatenation of the previous five items enables a clear positioning of the proposed design w.r.t the existing categories of works recalled in section 1.1. More precisely: we believe that DNNs-based solutions are incompatible with items 3, 4 and probably 5⁴. Machine learning solutions are not fully compatible with item 1 and it is not clear how to make it compatible with item 5. Moreover, the conclusion of [3] suggest that the non time-series specific nature of these approaches seems to penalize their performance in that specific context.

As for conventional methods sub-categories, leaving aside the forecasting-based approaches (item 3), we believe that the decomposition methods are more oriented by the shape of the time-series rather than the link between the temporal increments and the state configuration.

Two subcategories remain that are tightly linked to our proposal which are the control chart and the similarity search conventional approaches. The difference lies in the main role played by the sensors time increments in the construction of the associated *control charts*-like normality characterization proposed in this contribution and the strong multivariate character involved by opposition to the similarity based approaches mentioned in Section 1.1.1 which mainly concerns cyclic mono-variate time-series.

In the next section, the details of the proposed design methodology are given.

3. The proposed algorithm

Let us first introduce some notation that are extensively used in the sequel.

3.1. Notation

Given an integer $n \in \mathbb{N}$, the notation $\bar{n} := \{0, \dots, n - 1\}$ is used to denote the associated set of integers lower than n . We consider data including n_s sensors. The notation $s_t^{[i]}$ denotes the value of sensor i at instant t . When a time subset \mathcal{T} (that could be a single time-interval or a collection of time-intervals) is considered, the notation $\mathbf{s}_{\mathcal{T}}^{[i]}$ is used to refer to the time-series of sensor i over \mathcal{T} .

Given an integer $n_q \in \mathbb{N}$ with $n_q > 2$, an n_q -quantizer is a map $Q : \mathbb{R} \rightarrow \bar{n}_q := \{0, \dots, n_q - 1\}$ that associates an integer index \bar{n}_q to any real number. A typical way to *fit* a quantizer using a training data concerning sensor i is to determine a sequence of values v_k :

$$-\infty < v_0 < \dots < v_{n_q-2} < \infty \quad (1)$$

⁴Although batch learning solutions exist for NN, the impact of the updating on the weights and hence on the retro-compatibility of the newly updated model on the previous data needs to be carefully assessed.

that defines n_q disjoint time-intervals, namely:

$$(-\infty, v_0], (v_0, v_1], \dots, (v_{n_q-1}, \infty) \quad (2)$$

each of which can be labelled by an element of \bar{n}_q and such that the values belonging to the set $s_{\mathcal{T}}^{[i]}$ are uniformly distributed over the resulting intervals⁵.

Once such a quantizer $Q^{[i]}$ is defined for a sensor i , it is possible to create a quantized version $q_t^{[i]}$ of the associated time-series of sensor i , namely:

$$q_t^{[i]} = Q^{[i]}(s_t^{[i]}) \quad (3)$$

Moreover, given a time step $\Delta \in \mathbb{N}$, the quantized value Δ samples ahead $q_{t+\Delta}^{[i]}$ can be extracted. As a matter of fact, the pairs of the form:

$$c_t^{[i]} := (q_t^{[i]}, q_{t+\Delta}^{[i]}) \in \bar{n}_q^2 = \{0, \dots, n_q - 1\}^2 \quad (4)$$

play a crucial role in the proposed framework. Note that $c_t^{[i]}$ represents the **transition of sensor i** at instant t associated to the chosen step Δ which plays the role of hyper-parameter of the model. Note that for a given integer n_q the set of possible values of the transition $c_t^{[i]}$ is exactly $\bar{n}_q^2 := \{0, \dots, n_q - 1\}^2$ although for small sampling periods and small steps Δ , the number of truly encountered transitions is much smaller than n_q^2 should high values of n_q be used.

Remark 1 (the temptation of Markov chains).

Obviously, the quantization process and the definition of the transition pairs defined by (4) inevitably invokes the first step in the construction of Markov chains paradigm. Indeed, one can imagine a state defined by the vector of quantized values of all the sensors measurements which leads to a cardinality of $n_q^{n_s}$ for which the probability-of-transition matrix would be learned and used in the characterization of normality. This approach is not used in this contribution for three reasons: the first is linked to the scalability issue (we seek a solution that can be deployed even with industrial datasets that involve hundreds of sensors which leads to a prohibitive cardinality $n_q^{n_s}$ even for moderate quantization parameter n_q). The second reason is that the probability of transition is strongly linked to the type and especially the balance of the specific scenarios that are included in the training data (step changes, ramp tracking, etc.) while we seek a solution that is not so sensitive to the balance of contexts present in the training data. The last reason is that exploiting the anomaly in the probabilities requires observation over rather long time intervals which might induce important delays in the detection of anomalies. ♠

Instead of using Markov chains paradigm, the transition pairs defined in (4) are used hereafter to define clusters on which some properties are computed and used to characterize normality as explained later on.

Given a sensor i , a time interval \mathcal{T} and a transition $c \in \bar{n}_q^2$, the following set of instants is used in the sequel:

$$\bar{t}_c^{[i]}(\mathcal{T}) := \{t \in \mathcal{T} \mid c_t^{[i]} = c\} \quad (5)$$

namely, $\bar{t}^{[i]}(c, \mathcal{T})$ denotes the set of instants of \mathcal{T} from which the sensor i makes a transition equal to c .

An additional notation is needed to clearly describe the proposed approach. Given a discrete collection \mathbb{C} of vectors, say w_1, \dots, w_m of the same size n_w , namely:

$$\mathbb{C} := \{w_1, \dots, w_m\} \in 2^{\mathbb{R}^{n_w}} \quad (6)$$

An η -correlation remover is a set-valued map \mathcal{R}_η that extracts from \mathbb{C} a sub-collection of η -uncorrelated representative vectors, denoted by $\mathcal{R}_\eta(\mathbb{C})$ such that:

$$\begin{aligned} \forall w_i, w_j \in \mathcal{R}_\eta(\mathbb{C}) \\ (i \neq j) \quad \Rightarrow \quad |\text{corr}(w_i, w_j)| < \eta \end{aligned} \quad (7)$$

⁵The extreme values can be discarded by using robust standard scaler before computing the quantizing parameters for instance.

This operation helps reducing the cardinality of the collection \mathbb{C} by removing the correlated elements and leaving only a reduced number of representative elements of them. There are many possible efficient and rather straightforward implementations of such a map \mathcal{R}_η that are not mentioned here for the sake of brevity.

Finally, given a time-series $s_{\mathcal{T}}^{[i]}$ relative to a sensor i and given an integer $d \in \mathbb{N}$, the following sequence of time-series are optionally used:

$$s_{\mathcal{T}-i}^{[i,\Delta]} := [s_{\mathcal{T}-1}^{[i]}, \dots, s_{\mathcal{T}-(\Delta-1)}^{[i]}] \quad (8)$$

which represents the delayed version of $s_{\mathcal{T}}^{[i]}$ up to d previous samples. Note that in the above notation, the abuse of notation $\mathcal{T} - i$ is used to denote the sequence of instants obtained from the sequence \mathcal{T} by i -steps translation.

In the following development, each time the normality *viewed by a sensor i* is characterized (which involve all the other sensors as explained later), the delayed instances represented by $s_{\mathcal{T}-i}^{[i,d]}$ are appended as additional *virtual* sensors to form the extended set of sensors viewed by sensor i . Assuming that the same delay d is applied when each sensor's point of view is examined, the cardinality of the extended set of sensors becomes:

$$n_s^e := n_s + \Delta - 1 \quad (9)$$

and the set of indices of this extended is denoted by:

$$\bar{n}_s^e := \{0, \dots, n_s + \Delta - 1\} \quad (10)$$

in accordance with the already introduced notation at the beginning of this section. Before we dig into the details, it is mandatory that the overall architecture of the methodology can be grasped, namely:

Each sensor $i \in \bar{n}_s$ gives rise to 3 different characterizations of normality leading to 3 associated residuals. For each sensor i , these characterizations involve the following data:

$$[s_{\mathcal{T}}^{[j]}]_{j \in \bar{n}_s}, [s_{\mathcal{T}-i}^{[i,d]}]_{d \in \{1, \dots, \Delta-1\}} \quad (11)$$

namely, all the raw sensors time-series to which the delayed versions of the only i sensor, namely $s_{\mathcal{T}-i}^{[i,\Delta]}$ are added. Therefore, the total number of time-series used is $n_s^e = n_s + \Delta - 1$ and the elements being involved depend on i . Nevertheless, the following short notation is used to invoked these time-series:

$$[s_{\mathcal{T}}^{[j]}]_{j \in \bar{n}_s^e(i)} \quad (12)$$

very often the reference to i in $\bar{n}_s^e(i)$ is dropped using only \bar{n}_s^e when i is clear from the context without ambiguity.

Now that we have all that we need to describe the algorithm, let us precisely define the proposed parameters of normality. Notice that by normality parameters, we refer to those parameters that are involved in the computation of the normality indicators or residuals. They are the only parameters that one needs to keep in memory to represent what has been learnt from the training data. Once the normality parameters are defined, Section 3.3 shows how they are used to compute the associated residuals.

3.2. Building normality parameters from training data

Assume that a training dataset $\mathbb{D}_{\text{train}}$ is available that takes the following form:

$$\mathbb{D}_{\text{train}} := \left\{ s_{\mathcal{T}}^{[i]} \right\}_{i \in \bar{n}_s := \{1, \dots, n_s\}} \quad (13)$$

where \mathcal{T} is a collection of time intervals⁶. These measurements are first used to compute a set of n_q -quantizers $Q^{[i]}$, $i = 1, \dots, n_s$, one per sensor where n_q is some chosen integer⁷. This is done by first scaling the columns of the dataframe representing $\mathbb{D}_{\text{train}}$ and then by computing the parameters defining the quantization intervals (2) needed to define the quantizer maps⁸. This is done in step 1: of Algorithm 1 (see page 10).

Using these quantizers, the quantized versions $q_{\mathcal{T}}^{[i]}$, $q_{\mathcal{T}+\Delta}^{[i]}$ of the sensors time-series are computed together with the resulting transitions $c_{\mathcal{T}}^{[i]}$. This is done in step 2 of Algorithm 1.

From now on, the same computation are done for each sensor i leading to a **family of normality parameters (NP) indexed by the sensors**.

3.2.1. NP-1: The set of transitions

The first set of normality parameters viewed by sensor i is the set of transitions $c_{\mathcal{T}}^{[i]}$ itself. Indeed, a scenario involving a transition c_{new} at some time instant t_{new} that has never been seen in the training data might be considered as anomalous. Obviously, this unexpected event might be the result of an unseen context of use that is not included in the training data. A blind anomaly detector cannot distinguish between anomalies and unseen contexts. Here is where the operator feedback mentioned in the discussion of Section 1.2 comes into play. In the case of unseen context, handling the feedback amounts at adding the new transition to the normality set of transitions $c_{\mathcal{T}}^{[i]}$, namely:

$$c_{\mathcal{T}}^{[i]} \leftarrow c_{\mathcal{T}}^{[i]} \cup \{c_{\text{new}}\} \quad (14)$$

This is the reason why $\{c_{\mathcal{T}}^{[i]}\}_{i \in \bar{n}_s}$ is exported by Algorithm 1 as one of the normality parameters extracted from the training data \mathbb{D} .

3.2.2. NP-2: The clustered bounds on excursions

Given a sensor i and a normal transition $c \in c_{\mathcal{T}}^{[i]}$, **the bounds of the domains of variations of all the sensors (including the delayed version of sensor i 's time-series) that are compatible with this transition c is also viewed as normality parameter.** More precisely, for each pair (i, c) involving a sensor i and one of its *normal transitions*, say c , the following bounds are considered⁹:

$$\underline{b}_c^{[i]} := \left[\min_{t \in t_c^{[i]}(\mathcal{T})} s_r^{[j]} \right]_{j \in \bar{n}_s^e(i)} \in \mathbb{R}^{n_s^e} \quad (15a)$$

$$\bar{b}_c^{[i]} := \left[\max_{t \in t_c^{[i]}(\mathcal{T})} s_r^{[j]} \right]_{j \in \bar{n}_s^e(i)} \in \mathbb{R}^{n_s^e} \quad (15b)$$

More clearly, $\underline{b}_c^{[i]}$ is an n_s^e -dimensional vector in which the j -th component is the minimum value taken (in the training data) by sensor j over all instants at which, sensor i experienced the transition c . The same explanation holds for $\bar{b}_c^{[i]}$ except that it is the maximum value that is involved.

Note that the number of normality parameters involved depends on the number of transitions observed in the training data. More precisely, this involve the following number of new normality parameters:

$$n_b := 2 \cdot \sum_{i \in \bar{n}_s} \text{card}[c_{\mathcal{T}}^{[i]}] \quad (16)$$

⁶In the following developments, the special case where \mathcal{T} is a single interval corresponding to continuous recordings of the n_s sensors is sometimes implicitly used. The technicalities needed in the case where \mathcal{T} is a collection of such intervals are quite obvious and are sometimes omitted to keep the presentation simpler.

⁷Similar to Δ , this is another hyper parameter of model.

⁸In the `pandas` python-module for instance, this can be performed using the `pandas.cut` utility

⁹Note that the min and the max operator might represent robust version of the extreme values by using two extreme percentiles such as 1% and 99% for instance.

Now, if a *normal* transition c arises with violation of the above computed bounds at some instant t_{new} while the operator feedback tags it as normal, the updating of the normality parameters $\underline{b}_c^{[i]}$ and $\bar{b}_c^{[i]}$ can be easily done using the following updating rules where the min/max operators is to be applied component-wise:

$$\underline{b}_c^{[i]} \leftarrow \min\{\underline{b}_c^{[i]}, [s_{t_{\text{new}}}^{[j]}]_{j \in \bar{n}_s^e(i)}\} \quad (17a)$$

$$\bar{b}_c^{[i]} \leftarrow \max\{\bar{b}_c^{[i]}, [s_{t_{\text{new}}}^{[j]}]_{j \in \bar{n}_s^e(i)}\} \quad (17b)$$

On the other hand, if a new transition c_{new} that does not belong to the set of normal transitions $c_{\mathcal{T}}^{[i]}$ is encountered, then it is added to the set of *normal transition* as mentioned above [see (14)] and its associated bounds can be initialized using the current value of the n_s^e sensors as centers of the intervals while the width of the bounds associated to the nearest *normal transition* are used to define the bounds for the new transition.

3.2.3. NP-3: The clustered sensors configurations

The last set of normality parameters is given by the set of uncorrelated sensors's configurations for each given transition in the set of encountered transitions per sensor. More precisely, given a pair (i, c) of a sensor i and one of its *normal transitions* $c \in c_{\mathcal{T}}^{[i]}$, the following collection of n_s^e -dimensional vectors is considered:

$$\mathbb{C}_c^{[i]} := \underbrace{\{[s_t^{[j]}]_{j \in \bar{n}_s^e}\}_{t \in \mathcal{I}^{[i]}(\mathcal{T})}}_{w_t \in \mathbb{R}^{n_s^e}} \quad (18)$$

Note that each vector w_t in $\mathbb{C}_c^{[i]}$ represents the configurations, of the set of extended (by delays on sensor i) sensors when the transition c occurred on the sensor i at instant t . Since many of these vectors are highly correlated, the correlation remover map (see Section 3.1) is applied to the collection in order to build the new normality set of parameters associated to the pair (i, c) :

$$\mathbb{V}_c^{[i]} := \mathcal{R}_\eta(\mathbb{C}_c^{[i]}) \subset 2^{\mathbb{R}^{n_s^e}} \quad (19)$$

The cardinality of these sets cannot be determined a priori, however it is shown in Section 4 that after the application of the correlation remover \mathcal{R}_η this cardinality can generally be quite low. This suggests that the underlying physical laws combined with the transition-induced clusters reduce the number of really different (uncorrelated) configurations of the sensors for a given transition. The computation of (19) is performed in step 3.2 of Algorithm 1.

As it is explained hereafter when the computation of the residuals is discussed, the normality induced by the elements of $\mathbb{V}_c^{[i]}$ is determined as follows: when the transition c is encountered on sensor i at some instant t_{new} , a *normal situation* corresponds to the presence, in $\mathbb{V}_c^{[i]}$ of at least one highly correlated element with the current sensors configurations $[s_{t_{\text{new}}}^{[j]}]_{j \in \bar{n}_s^e}$. If this is not the case while the operator labels the situation as normal, then handling the feedback amounts at adding the current sensors configuration $[s_{t_{\text{new}}}^{[j]}]_{j \in \bar{n}_s^e}$ to $\mathbb{V}_c^{[i]}$, namely:

$$\mathbb{V}_c^{[i]} \leftarrow \mathbb{V}_c^{[i]} \cup \{[s_{t_{\text{new}}}^{[j]}]_{j \in \bar{n}_s^e}\} \quad (20)$$

Notice that if several instants $\{t_k\}_{k=1}^m$ correspond to False Positive diagnosis according to the operator feedback, then the corresponding multi-instances feedback can be handled by simply adding all the corresponding instances to the original set and applying the correlation remover over the resulting augmented set, namely:

$$\mathbb{V}_c^{[i]} \leftarrow \mathcal{R}_\eta\left(\mathbb{V}_c^{[i]} \bigcup_{k=1}^m \{[s_{t_k}^{[j]}]_{j \in \bar{n}_s^e}\}\right) \quad (21)$$

All the above developments can be summarized by Algorithm 1:

ALGORITHM 1: FIT THE MODEL

Given: $\mathbb{D}_{\text{train}}$ [see (13)], n_q , Δ , η

- 1: Compute the n_q quantizers $Q^{[i]}$ for $i = 1, \dots, n_s$
- 2: Compute the transitions $c_{\mathcal{T}}^{[i]}$ for $i = 1, \dots, n_s$
- 3: **For** $i = 1, \dots, n_s$
 - 3.1: Compute $b_c^{[i]}$ and $\bar{b}_c^{[i]}$ for $c \in c_{\mathcal{T}}^{[i]}$ using (15)
 - 3.2: Compute $\nabla_c^{[i]}$ for $c \in c_{\mathcal{T}}^{[i]}$ using (18)-(19)

Output: $\{c_{\mathcal{T}}^{[i]}\}_{i \in \bar{n}_s}$, $\{b_c^{[i]}, \bar{b}_c^{[i]}, \nabla_c^{[i]}\}_{c \in c_{\mathcal{T}}^{[i]}\}_{i \in \bar{n}_s}$

3.3. Computing the residuals

Associated to the normality parameters defined in sections 3.2.1, 3.2.2 and 3.2.3, three associated residuals are defined for a better explainability of the anomalous time-series. The residuals are computed for time-series that last over a time windows including N successive measurements. note that in order for the underlying time window to contain at least one transition, the constraint $N > \Delta$ should ne respected. Notice that for any choice of $N \geq \Delta$ it is possible to compute the associated residuals by using the same normality parameters introduced in Section 3.2. The window length plays the role of *aggregating* parameter that can be adapted to the presumed time scale of the faults visibility and remanence.

The three residuals are respectively denoted by r_{trans} (transition), r_{bound} (bounds) and r_{conf} (configurations) since they are expected to reveal three different kinds of anomalies consequences.

3.3.1. Anomalous transitions-related residual r_t

Denoting by \mathcal{T}_p the interval over which the residuals are to be predicted and consisting of N sampling instants, the residual r_t associated to anomalous transitions is defined as follows:

$$r_{\text{trans}} := \frac{1}{n_s N} \sum_{i \in \bar{n}_s} \text{card}\{t \in \mathcal{T}_p \mid c_t^{[i]} \notin c_{\mathcal{T}_{\text{train}}}^{[i]}\} \quad (22)$$

where $N := \text{card}(\mathcal{T}_p)$ and $c_{\mathcal{T}_{\text{train}}}^{[i]}$ is the set of *normal* transitions computed using the training data and the following operator labelling feedback. More clearly, the residual r_t corresponds to the normalized¹⁰ number of *anomalous transitions* (observed at instants $t \in \mathcal{T}_p$ belonging to the prediction time window). Notice that anomalous transition can be raised following a context of use that involves rapid transitions that were not present in the training data. But it can be also true that these unexpected transition are the result of faults impacting the parameters of the equipment.

Note that although the residual r_t is computed by adding and normalizing the number of anomalous transitions, it is obviously possible to keep track of the indices i and t that are involved in the computation so that more specific explanation can be provided (which transition on which sensor at which instant contributed to the residual potential burst).

3.3.2. Anomalous domain-related residual r_b

Contrary to r_t , the residual r_b corresponds to normal transitions c for a sensor i for which anomalous values of some sensors in the extended set of sensors¹¹ are observed. Namely, these anomalous values do not belong to the

¹⁰w.r.t the number of sensors and the length of the prediction interval \mathcal{T}_p

¹¹Viewed by sensor i : this includes all the original sensors to which the delayed versions of sensor i are added.

domains defined by the normality parameters $\underline{b}_c^{[i]} \in \mathbb{R}^{n_s^e}$ and $\bar{b}_c^{[i]} \in \mathbb{R}^{n_s^e}$ for that specific transition c .

More rigorously, this residual is defined by:

$$r_{\text{bound}} := \frac{1}{n_s \cdot N} \sum_{i \in \bar{n}_s} \sum_{t \in \mathcal{T}_p} \delta^{[i]}(t) \quad (23)$$

$$\delta^{[i]}(t) := \frac{1}{n_s + \Delta - 1} \text{distance}([s_t^{[j]}]_{j \in n_s^e}, [\underline{b}_{c_t^{[i]}}^{[i]}, \bar{b}_{c_t^{[i]}}^{[i]}]) \quad (24)$$

Notice that the r.h.s of (24) represents the distance between a vector in $\mathbb{R}^{n_s^e}$, namely $[s_t^{[j]}]_{j \in n_s^e}$ and the normal hypercube in $\mathbb{R}^{n_s^e}$ which is define by the second argument $[\underline{b}_{c_t^{[i]}}^{[i]}, \bar{b}_{c_t^{[i]}}^{[i]}]$. This distance can be derived in a straightforward manner from any scalar distance between a real ξ and a scalar interval $[\underline{\xi}, \bar{\xi}]$ such as the one defined by:

$$\text{distance}(\xi, [\underline{\xi}, \bar{\xi}]) := \left[\frac{\max\{0, \underline{\xi} - \xi\} + \max\{0, \xi - \bar{\xi}\}}{\bar{\xi} - \underline{\xi} + \varepsilon} \right]^\nu$$

for some integer $\nu \in \mathbb{N}$. When this residual takes non-zero values, it underlines that during some normal transition, at least a sensor (say j) took values that are outside the normal domain observed in the training dataset. This can be an indicator of some *change in the transfer (gain) coefficient involving the way the sensor j appears in the r.h.s of the unknown physical relationship that governs the increments of sensor i* . Notice that, here again, although the residual r_b defined by (23)-(24) is a global indicator of anomaly, its individual components (i, j, t) can be traced back to induce explainable diagnosis.

3.3.3. Anomalous configuration-related residual

The last residual r_{conf} is oriented towards the detection of changes in the relative configurations of the different sensors (including the additional delay related ones) for given set of transitions affecting the different original sensors. As explained in Section 3.2.3, for a given sensor i experimenting a transition $c = c_t^{[i]}$ at some instant t , the normality means that there is a vector in $\mathbb{V}_c^{[i]} \subset \mathbb{R}^{n_s^e}$ which is highly correlated to the current measurement vector $\{s_t^{[j]}\}_{j \in \bar{n}_s^e}$. This suggests the following definition of r_{conf} :

$$r_{\text{conf}} := \frac{1}{(n_s + \Delta - 1)N} \sum_{i \in \bar{n}_s} \sum_{t \in \mathcal{T}_p} \left[1 - \max_{v \in \mathbb{V}_c^{[i]}} \{\text{corr}([s_t^{[j]}]_{j \in \bar{n}_s^e}, v)\} \right] \quad (25)$$

in which c is used in $\mathbb{V}_c^{[i]}$ to shortly refer to $c_t^{[i]}$.

Obviously, this residual is expected to reveal a change in the relative configuration of sensor inducing the same increment on the sensor i . Since a summation on i is used, the residuals account for any change of the unknown underlying relationships governing all the involved dynamics.

4. Illustrative examples

In this section, the behavior of the residuals generated by the above described algorithm is first examined for a specific setting of the hyper-parameters before an extended statistical comparison with some other algorithms is analyzed in Section 5.

4.1. Example 1: Detecting slight parameter changes in Lorentz attractors

In the first example¹², the ability of the proposed framework to detect slight parameters change in a dynamical system is investigated. To do so, the following well known Lorentz model is used:

$$\dot{x}_1 = \sigma(x_2 - x_1) \quad (26a)$$

$$\dot{x}_2 = x_1(\rho - x_3) - x_2 \quad (26b)$$

$$\dot{x}_3 = x_1x_2 - \beta x_3 \quad (26c)$$

where σ , ρ and β are the parameters that might be affected by unpredictable changes one would like to detect thanks to the anomaly detector using the two measurement sensors defined by $s_1 = x_1$ and $s_2 = x_3$, namely

$$s := [x_1, x_3]$$

The nominal values of the parameters are given by $\sigma = 12$, $\rho = 28$ and $\beta = 8/3$.

The working time-series are depicted on Figure 2 where six different intervals of time-series are concatenated, each of which is generated using different initial conditions and different values of the parameters. More precisely, the green intervals on Figure 2 correspond to nominal values of the parameters while different initial states is used leading to obviously different time-series because of the very nature of the oscillator which is not open-loop asymptotically stable. The red regions correspond to different detuned sets of parameters as shown in the last row of plots where the evolution of the three parameters are shown after normalizing by the nominal values mentioned above (Hence 1 corresponds to the nominal values). To be more precise, in the first anomalous region (third interval), σ takes a value that is 30% lower than the nominal value (8 instead of 12). In the second anomalous interval (the fifth interval), the ρ parameter is 7% lower than the nominal value (26 instead of 28) while the last interval shows β taking 25% above the nominal value (10/3 instead of 8/3). Note that these relatively small changes are chosen in order to get raw time-series that cannot easily be distinguishable as it can be observed in Figure 2 .

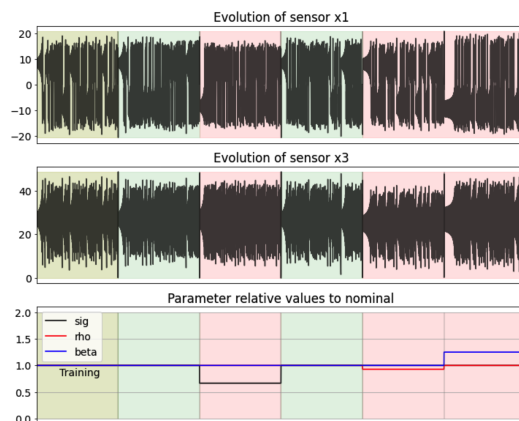


Figure 2: **Example 1:** Time-series representing the two sensors evolution and the associated evolution of the model's parameters.

The time-series are obtained by simulating (26) using 4th-order Runge-Kutta method with a sampling period of 10^{-2} . As for the anomaly detector setting, the following set of hyper parameters are used:

$$n_q = 20, \quad \Delta = 20, \quad \eta = 0.95 \quad \nu = 1 \quad (27)$$

The residuals delivered by the fitted anomaly detector using a window of length $N = 100$ are shown in Figure 3 which clearly show that over each of the anomalous regions, at least one of the residual is clearly above the level it takes over the normal regions.

¹²The dataset used in this example is accessible at <https://github.com/mazenalamir/lorentz-attractor-blind-fault-detection-dataset>

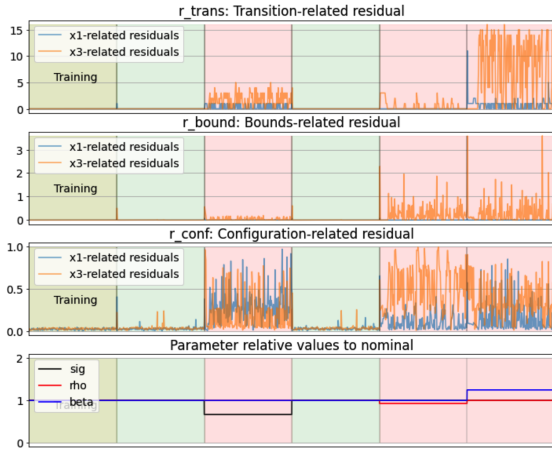


Figure 3: Evolution of the family of residuals viewed by sensor x_1 and x_3 when both sensors are available for the construction of the anomaly detector associated to the hyper-parameters given by (27).

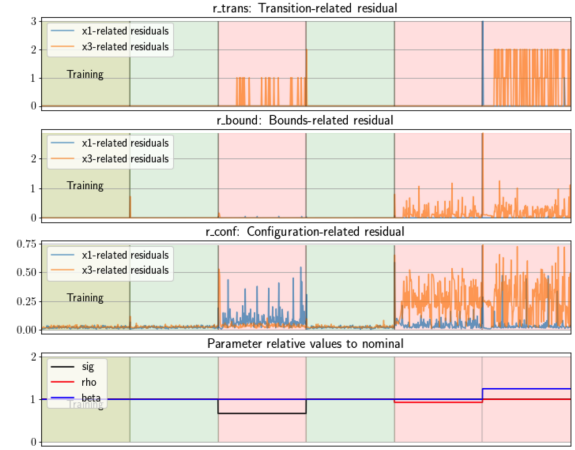


Figure 4: **Example 1:** Evolution of the family of residuals viewed by sensor x_1 and x_3 when both sensors are available for the construction of the anomaly detector associated to the hyper-parameters given by (27) **except that** $n_q = 8$ is used. Instead of 20.

An interesting feature that can be observed is the high sensitivity of the transition residual r_{trans} viewed by sensor x_3 when the parameter β is anomalous. This simply reflects (26c) which clearly involves a direct impact of β on the transitions of sensor s_3 . It is also noticeable that for this example and as long as the associated relatively small changes introduced on the model parameters are concerned, the bound-related residual r_{bound} viewed by sensor x_1 does not reveal any anomalies while the configuration-related residuals r_{conf} viewed by both sensors are sensitive to all anomalies.

Figure 5 shows the statistics of the cardinalities of the sets of configurations $\mathbb{V}_c^{[x_1]}$ and $\mathbb{V}_c^{[x_3]}$ among the 281 transitions of quantized x_1 and the 311 transitions of the quantized x_3 . Notice that the majority of the cases corresponds to a single vector and that the cardinality rarely goes beyond 6 while the elements of these sets lie in \mathbb{R}^{21} (since $n_s^e = n_s + \Delta - 1 = 2 + 20 - 1 = 21$).

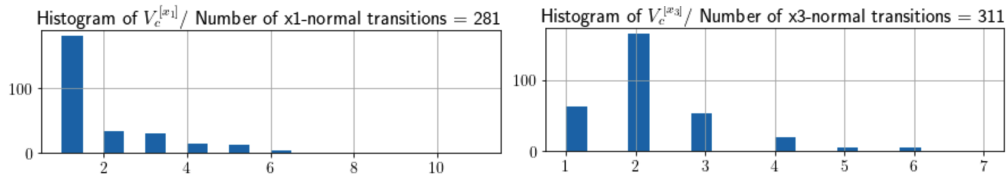


Figure 5: **Example 1:** Histograms of the cardinalities of the fitted sets of configurations $\mathbb{V}_c^{[x_1]}$ and $\mathbb{V}_c^{[x_3]}$ among the 281 transitions of quantized x_1 and the 311 transitions of the quantized x_3 . The anomaly detector's hyper-parameters are given by (27).

Notice that these cardinalities are intimately linked to the correlation threshold being used, namely $\eta = 0.95$. Finally, in order to appreciate the impact of the choice of the quantization parameter n_q , the same results as the ones shown in figures 3 and 5 are given in the case where $n_q = 8$ is used instead of $n_q = 20$. This leads to the results shown in Figures 4 and 6.

Notice that the detection is still possible although r_{trans} increase is far less important suggesting a possible sensitivity of the success to random factors. But on the other hand, the detection of changes in σ is now more clearly associated to the transition on x_1 as it is obvious from (26a). On the other hand, the residual of the green normal regions show also less burst leading to less potential false positive diagnosis. This discussion clearly underlines that n_q is a hyper parameter to be finely tuned in the design process. Figure 6 shows the obvious fact that when less

- [22] Bernhard Schölkopf, John C Platt, John Shawe-Taylor, Alex J Smola, and Robert C Williamson. Estimating the support of a high-dimensional distribution. *Neural computation*, 13(7):1443–1471, 2001.
- [23] Arnaldo Sgueglia, Andrea Di Sorbo, Corrado Aaron Visaggio, and Gerardo Canfora. A systematic literature review of iot time series anomaly detection solutions. *Future Generation Computer Systems*, 134:170–186, 2022.
- [24] Kamran Shaukat, Talha Mahboob Alam, Suhuai Luo, Shakir Shabbir, Ibrahim A Hameed, Jiaming Li, Syed Konain Abbas, and Umair Javed. A review of time-series anomaly detection techniques: A step to future perspectives. In *Advances in Information and Communication: Proceedings of the 2021 Future of Information and Communication Conference (FICC), Volume 1*, pages 865–877. Springer, 2021.
- [25] Naoya Takeishi and Takehisa Yairi. Anomaly detection from multivariate time-series with sparse representation. In *2014 IEEE International Conference on Systems, Man, and Cybernetics (SMC)*, pages 2651–2656. IEEE, 2014.
- [26] William H Woodall and Matoteng M Ncube. Multivariate cusum quality-control procedures. *Technometrics*, 27(3):285–292, 1985.
- [27] Yue Wu, Yinpeng Chen, Lijuan Wang, Yuancheng Ye, Zicheng Liu, Yandong Guo, and Yun Fu. Large scale incremental learning. In *Proceedings of the IEEE/CVF Conference on Computer Vision and Pattern Recognition*, pages 374–382, 2019.
- [28] Chin-Chia Michael Yeh, Yan Zhu, Liudmila Ulanova, Nurjahan Begum, Yifei Ding, Hoang Anh Dau, Diego Furtado Silva, Abdullah Mueen, and Eamonn Keogh. Matrix profile i: all pairs similarity joins for time series: a unifying view that includes motifs, discords and shapelets. In *2016 IEEE 16th international conference on data mining (ICDM)*, pages 1317–1322. Ieee, 2016.
- [29] Yue Zhao, Zain Nasrullah, and Zheng Li. Pyod: A python toolbox for scalable outlier detection. *Journal of Machine Learning Research*, 20(96):1–7, 2019.
- [30] Anatoly Zhigljavsky. Singular spectrum analysis for time series: Introduction to this special issue. *Statistics and its Interface*, 3(3):255–258, 2010.
- [31] Bo Zong, Qi Song, Martin Renqiang Min, Wei Cheng, Cristian Lumezanu, Daeki Cho, and Haifeng Chen. Deep autoencoding gaussian mixture model for unsupervised anomaly detection. In *International conference on learning representations*, 2018.